Acta Crystallographica Section C
Crystal Structure Communications
ISSN 0108-2701

Two similarly substituted benzo[*h*]-pyrazolo[3,4-*b*]quinoline-5,6(10*H*)-diones: supramolecular structures in two and three dimensions

Yurina Díaz,[a] Jairo Quiroga,[a] Justo Cobo[b] and Christopher Glidewell[c]*

[a]Departamento de Química, Universidad de Valle, AA 25360 Cali, Colombia, [b]Departamento de Química Inorgánica y Orgánica, Universidad de Jaén, 23071 Jaén, Spain, and [c]School of Chemistry, University of St Andrews, Fife KY16 9ST, Scotland
Correspondence e-mail: cg@st-andrews.ac.uk

Received 22 April 2010
Accepted 18 May 2010
Online 26 May 2010

The molecules of 8-methyl-7,10-diphenyl-5*H*-benzo[*h*]pyrazolo[3,4-*b*]quinoline-5,6(10*H*)-dione, $C_{27}H_{17}N_3O_2$, (I), are weakly linked into chains by a single C—H···O hydrogen bond, and these chains are linked into sheets by a π–π stacking interaction involving pyridyl and aryl rings. In 8-methyl-7-(4-methylphenyl)-10-phenyl-5*H*-benzo[*h*]pyrazolo[3,4-*b*]quinoline-5,6(10*H*)-dione, $C_{28}H_{19}N_3O_2$, (II), the molecules are linked into a three-dimensional framework structure by a combination of C—H···N, C—H···O and C—H···π(arene) hydrogen bonds, together with a π–π stacking interaction analogous to that in (I).

Comment

We are interested in the synthesis and biological properties of new pyrazolo[3,4-*b*]quinoline derivatives, some of which have exhibited parasiticidic properties (Bristol–Meyers Co., 1973), bactericidal activity (Farghaly *et al.*, 1989) and vasodilator properties (Bell & Ackerman, 1990), while some have been evaluated for enzymatic inhibitory activity (Gatta *et al.*, 1991). We have directed much of our work in this area towards the synthesis of such compounds using three-component reactions between 5-aminopyrazoles, aromatic aldehydes and ketones containing active methylene units. We report here the structures of two closely-related benzo[*h*]pyrazolo[3,4-*b*]quinoline-5,6(10*H*)-diones, namely 8-methyl-7,10-diphenyl-5*H*-benzo[*h*]-pyrazolo[3,4-*b*]quinoline-5,6(10*H*)-dione, (I), and 8-methyl-7-(4-methylphenyl)-10-phenyl-5*H*-benzo[*h*]pyrazolo[3,4-*b*]quinoline-5,6(10*H*)-dione, (II) (Figs. 1 and 2), which were prepared using naphthalene-1,2,4(3*H*)-trione as the methylene-active ketone component (see scheme). It turned out that these structure determinations were essential for the unambiguous identification of these compounds, because it was not possible using the normal spectroscopic techniques to determine the regiochemistry of the synthetic reactions and, in particular, to distinguish thereby between the benzo[*h*]pyrazolo[3,4-*b*]-quinolinedione structures actually formed and the possible isomeric benzo[*g*]pyrazolo[3,4-*b*]quinolinediones, which had been expected on the basis of a recent report (Chen *et al.*, 2008).

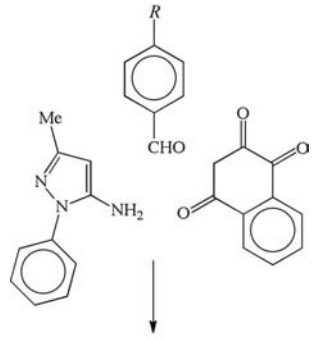

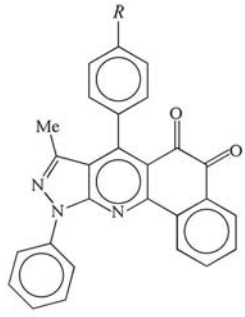

(I) R = H
(II) R = Me

Although the constitutions of (I) and (II) differ only in the presence of a 4-methyl substituent in the C71–C76 aryl ring in (II), these two compounds crystallize in different crystal systems, *viz.* monoclinic and triclinic, respectively. They also exhibit very different modes of supramolecular aggregation, in the form of sheets built from π-stacked hydrogen-bonded chains in (I) compared with a complex three-dimensional framework structure in (II). On the other hand, the corresponding intramolecular bond distances are very similar in the two compounds with, in each case, a long C5—C6 bond between the two adjacent carbonyl groups (Table 1), as is typical for such structural units (Allen *et al.*, 1987). There is clear evidence for bond fixation in the pyrazole ring, with typical aromatic-type delocalization in the pyridine ring and in the terminal carbocyclic ring of the fused ring system (*cf.* scheme).

The only significant differences between the molecular structures of (I) and (II) are to be found in their conformations, as defined by the torsion angles (Table 1) defining the orientations of the two pendent aryl rings relative to the fused polycyclic core of the molecules. In both compounds, the carbocyclic ring (C4a/C5/C6/C6a/C11a/C11b) is slightly distorted towards an envelope conformation, folded across the line C5···C6a, slightly more markedly in (II) than in (I); in (I), the maximum deviation from the mean plane described by the

 doi:10.1107/S0108270110018500

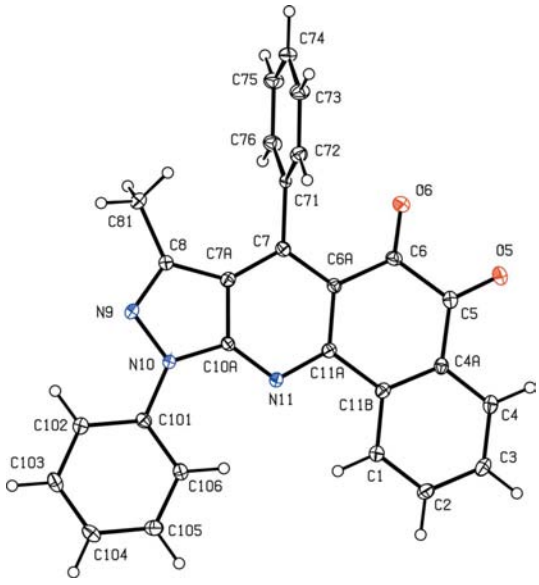

Figure 1
The molecular structure of (I), showing the atom-labelling scheme. Displacement ellipsoids are drawn at the 30% probability level and H atoms are shown as small spheres of arbitrary radii.

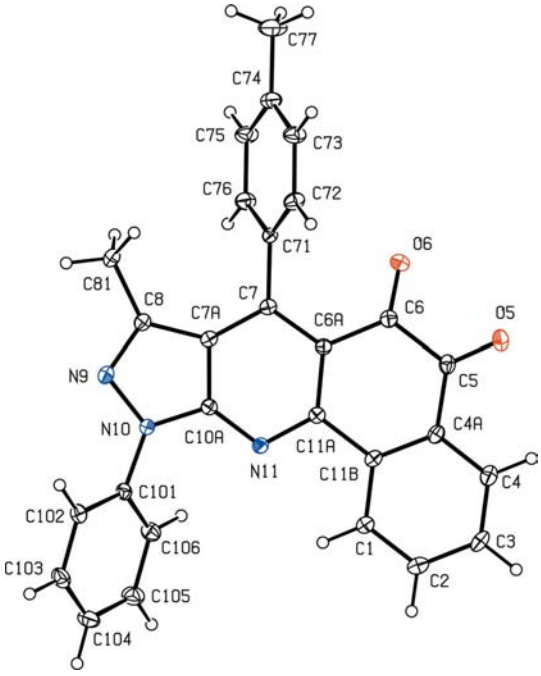

Figure 2
The molecular structure of (II), showing the atom-labelling scheme. Displacement ellipsoids are drawn at the 30% probability level and H atoms are shown as small spheres of arbitrary radii.

ring atoms is 0.046 (2) Å for atom C6, but in (II), the maximum deviation is 0.072 (2) Å, again for atom C6. This ring distortion is reflected in, and possibly caused by, the nonparallel orientation of the two carbonyl groups (Table 1), itself probably resulting from the mutual repulsion of the two negatively polarized O atoms.

The crystal structure of (I) contains just one rather weak C—H···O hydrogen bond, while intermolecular C—H···N and C—H···π interactions are absent. The hydrogen bond links molecules which are related by the 2_1 screw axis along $(0, y, -\frac{1}{4})$ into a $C(6)$ (Bernstein *et al.*, 1995) chain running parallel to the [010] direction (Fig. 3). Chains of this type are linked into sheets by means of a π–π stacking interaction. The plane of the pyridine ring of the molecule at (x, y, z), which forms part of the $C(6)$ chain along $(0, y, -\frac{1}{4})$, makes a dihedral angle of only 2.66 (2)° with the plane of the C101–C106 aryl ring in the molecule at $(x, \frac{1}{2}-y, -\frac{1}{2}+z)$, which itself forms part of the $C(6)$ chain along $(0, y, -\frac{3}{4})$. The interplanar spacing between these two rings is *ca* 3.38 Å, with a ring-centroid separation of 3.601 (2) Å, corresponding to a ring-centroid offset of *ca* 1.28 Å. In this manner, the reference chain along $(0, y, -\frac{1}{4})$ is linked to the two adjacent chains along $(0, y, -\frac{3}{4})$ and $(0, y, \frac{1}{4})$, so forming a sheet of π-stacked hydrogen-bonded chains lying parallel to (100) (Fig. 3).

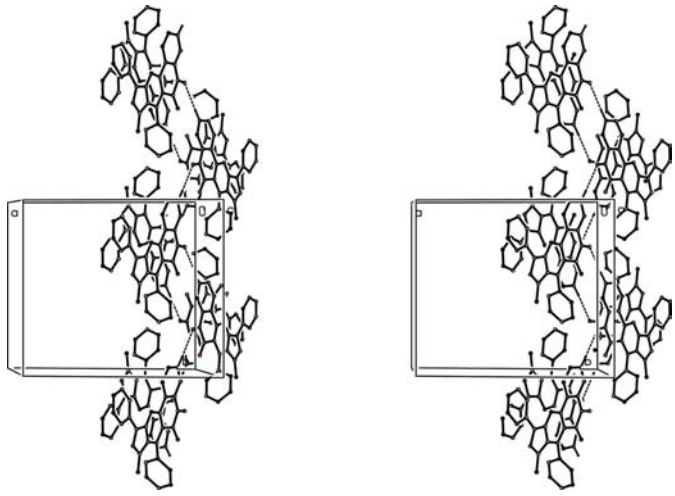

Figure 3
A stereoview of part of the crystal structure of (I), showing the π-stacking of the hydrogen-bonded $C(6)$ chains along $(0, y, -\frac{1}{4})$ and $(0, y, -\frac{3}{4})$ to form part of the π-stacked sheet parallel to (100). Dashed lines indicate hydrogen bonds. For the sake of clarity, H atoms not involved in the motif shown have been omitted.

The three-dimensional framework structure of (II) is built from a combination of C—H···N, C—H···O and C—H···π(arene) hydrogen bonds (Table 2), together with a π–π stacking interaction similar to that found in (I). Despite the complexity of the framework, its formation can readily be analysed using the substructure approach (Ferguson *et al.*, 1998*a*,*b*; Gregson *et al.*, 2000). In particular, an inversion-related pair of C—H···N hydrogen bonds (Table 2) links an inversion-related pair of molecules into a cyclic centrosymmetric $R_2^2(14)$ dimer centred at $(\frac{1}{2}, \frac{1}{2}, \frac{1}{2})$. This finite zero-dimensional substructural fragment can be regarded as the key building block in the overall structure, as the other three interactions, acting individually, link dimers of this type to form three distinct one-dimensional substructures. It is convenient to consider the actions of each of the other three intermolecular interactions in turn, both when acting alone and when acting to link the $R_2^2(14)$ dimers.

When acting alone, the C—H···O hydrogen bond links molecules related by translation to form a $C(12)$ chain running

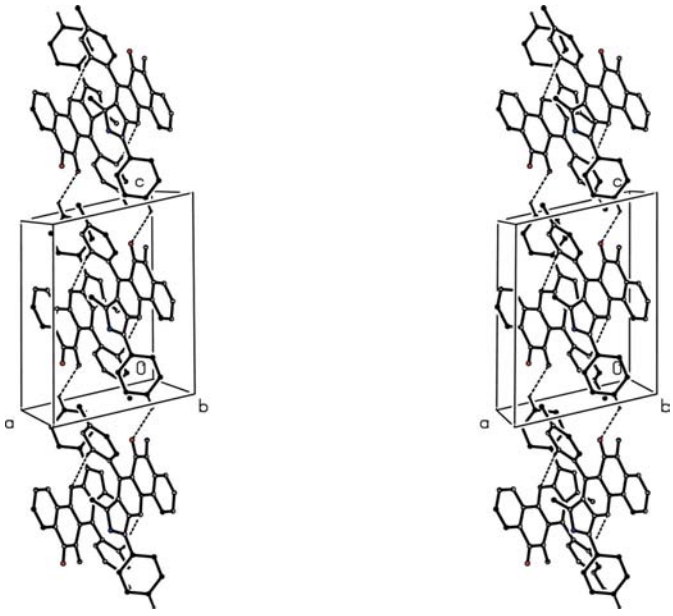

Figure 4
A stereoview of part of the crystal structure of (II), showing the formation of a hydrogen-bonded chain of alternating $R_2^2(14)$ and $R_4^4(30)$ rings along [001], built from C—H···N and C—H···O hydrogen bonds (dashed lines). For the sake of clarity, H atoms not involved in the motifs shown have been omitted.

parallel to the [001] direction. When acting in concert with the C—H···N hydrogen bond, the C—H···O interaction links $R_2^2(14)$ dimers into a chain of rings along [001] in which $R_2^2(14)$ rings centred at $(\frac{1}{2}, \frac{1}{2}, \frac{1}{2} + n)$, where n represents an integer, alternate with $R_4^4(30)$ rings centred at $(\frac{1}{2}, \frac{1}{2}, n)$, where n again represents an integer (Fig. 4). The C—H···π(arene) hydrogen bond links the molecules at (x, y, z) and $(1 - x, 1 - y, 1 - z)$ into a centrosymmetric dimer and, in combination with the C—H···N hydrogen bond, generates a chain of centrosymmetric rings running parallel to the [010] direction, with $R_2^2(14)$ rings built from paired C—H···N hydrogen bonds centred at $(\frac{1}{2}, \frac{1}{2} + n, \frac{1}{2})$ alternating with rings built from paired C—H···π(arene) hydrogen bonds centred at $(\frac{1}{2}, n, \frac{1}{2})$, where in both cases n represents an integer (Fig. 5). The pyridine ring of the molecule at (x, y, z) and the fused aryl ring of the molecule at $(2 - x, 1 - y, 1 - z)$ are almost parallel, with a dihedral angle between their mean planes of only 3.36 (2)°. The ring-centroid separation is 3.723 (2) Å and the interplanar spacing is *ca* 3.42°, corresponding to a ring-centroid offset of *ca* 1.47 Å. The effect of this π–π stacking interaction is to link the hydrogen-bonded $R_2^2(14)$ dimers into a π-stacked chain of dimers running parallel to the [100] direction (Fig. 6).

In the structure of (II) it is thus possible to identify three distinct substructural chains along [100], [010] and [001], each utilizing a different pair of direction-specific intermolecular interactions. The combination of these three substructural motifs generates a three-dimensional framework structure of considerable complexity.

Thus, the notional replacement of a single H atom in (I) by a methyl group in (II) is associated with a change in crystal system, with differences in the overall molecular conformations, in particular the dihedral angles between the polycyclic ring system and the pendent rings (*cf.* Table 1), and with a major change in the supramolecular aggregation and the molecular packing. The direction-specific intermolecular forces which influence the molecular arrangements in the structures of (I) and (II) are comparatively weak, and the interpretation and prediction of crystal structures dominated by such forces, as opposed to the much stronger forces between charged entities, remains problematic, especially in molecules such as those of (I) and (II) having some degree of conformational flexibility (Day *et al.*, 2009). Any attempt to provide a simple explanation for the observed differences between the structures of (I) and (II) is likely, at the present stage, to be entirely speculative.

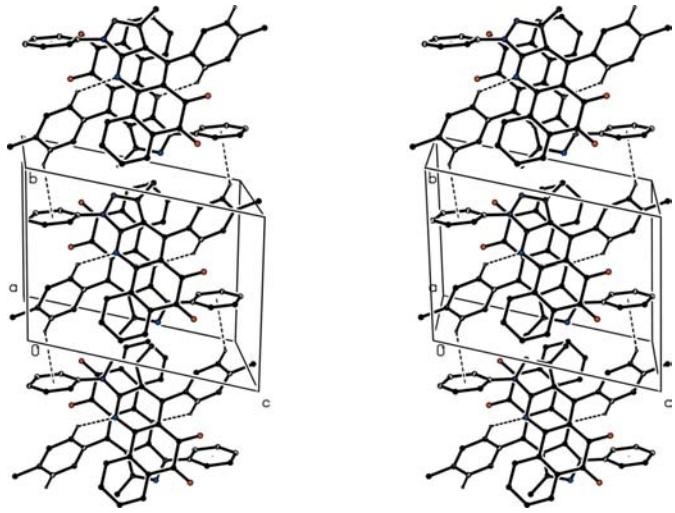

Figure 5
A stereoview of part of the crystal structure of (II), showing the formation of a hydrogen-bonded chain of centrosymmetric rings along [010], built from C—H···N and C—H···π(arene) hydrogen bonds (dashed lines). For the sake of clarity, H atoms not involved in the motifs shown have been omitted.

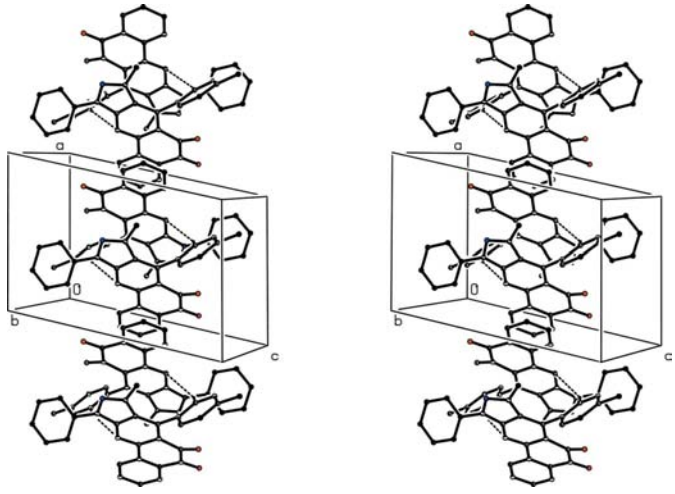

Figure 6
A stereoview of part of the crystal structure of (II), showing the formation of a π-stacked chain of hydrogen-bonded dimers along [100]. Dashed lines indicate hydrogen bonds. For the sake of clarity, H atoms not involved in the motif shown have been omitted.

Experimental

An intimate mixture containing 1 mmol of each of naphthalene-1,2,4(3*H*)-trione, 5-amino-3-methyl-1-phenylpyrazole and the appropriate aldehyde [benzaldehyde for (I) or 4-tolualdehyde for (II)] was irradiated in a microwave oven in the absence of solvent for 3 min. The solids obtained were purified by recrystallization from ethanol, and crystals suitable for single-crystal X-ray diffraction were grown by slow evaporation of solutions in dimethylformamide. Analysis for (I): orange crystals, yield 85%, m.p. 545–546 K; MS *m*/*z* (%): 415 (M^+, 19), 386 (100), 77 (6). Analysis for (II): red crystals, yield 85%, m.p. 546–547 K; MS *m*/*z* (%): 429 (M^+, 24), 414 (15), 400 (100) 386 (95).

Compound (I)

Crystal data

$C_{27}H_{17}N_3O_2$
M_r = 415.44
Monoclinic, $P2_1/c$
a = 15.436 (5) Å
b = 13.622 (7) Å
c = 9.359 (5) Å
β = 105.00 (4)°
V = 1900.9 (16) Å^3
Z = 4
Mo $K\alpha$ radiation
μ = 0.09 mm^{-1}
T = 120 K
0.27 × 0.12 × 0.10 mm

Data collection

Bruker–Nonius KappaCCD area-detector diffractometer
Absorption correction: multi-scan (*SADABS*; Sheldrick, 2003)
T_{min} = 0.956, T_{max} = 0.991
20384 measured reflections
3532 independent reflections
2660 reflections with $I > 2\sigma(I)$
R_{int} = 0.050

Refinement

$R[F^2 > 2\sigma(F^2)]$ = 0.049
$wR(F^2)$ = 0.106
S = 1.11
3532 reflections
290 parameters
H-atom parameters constrained
$\Delta\rho_{max}$ = 0.20 e Å^{-3}
$\Delta\rho_{min}$ = −0.24 e Å^{-3}

Compound (II)

Crystal data

$C_{28}H_{19}N_3O_2$
M_r = 429.46
Triclinic, $P\overline{1}$
a = 8.9952 (15) Å
b = 9.6201 (15) Å
c = 12.537 (4) Å
α = 98.72 (2)°
β = 103.31 (2)°
γ = 95.48 (2)°
V = 1033.9 (4) Å^3
Z = 2
Mo $K\alpha$ radiation
μ = 0.09 mm^{-1}
T = 120 K
0.39 × 0.34 × 0.10 mm

Data collection

Bruker–Nonius KappaCCD area-detector diffractometer
Absorption correction: multi-scan (*SADABS*; Sheldrick, 2003)
T_{min} = 0.963, T_{max} = 0.991
24512 measured reflections
3849 independent reflections
2820 reflections with $I > 2\sigma(I)$
R_{int} = 0.056

Refinement

$R[F^2 > 2\sigma(F^2)]$ = 0.052
$wR(F^2)$ = 0.115
S = 1.08
3849 reflections
300 parameters
H-atom parameters constrained
$\Delta\rho_{max}$ = 0.24 e Å^{-3}
$\Delta\rho_{min}$ = −0.29 e Å^{-3}

All H atoms were located in difference maps and subsequently treated as riding atoms in geometrically idealized positions, with C—H = 0.95 (aromatic) or 0.98 Å (methyl) and with U_{iso}(H) = kU_{eq}(C), where k = 1.5 for the methyl groups, which were permitted to rotate but not to tilt, and 1.2 for all other H atoms.

Table 1
Comparison of selected geometric parameters (Å, °) in (I) and (II).

	(I)	(II)
C5—C6	1.527 (3)	1.530 (3)
C7a—C8	1.423 (3)	1.423 (3)
C8—N9	1.303 (2)	1.316 (3)
N9—N10	1.377 (2)	1.377 (2)
N10—C10a	1.364 (2)	1.349 (2)
C10a—C7a	1.396 (3)	1.394 (3)
C6a—C7—C71—C72	−85.8 (2)	−67.4 (3)
N9—N10—C101—C102	11.4 (3)	−47.3 (3)
O5—C5—C6—O6	9.4 (3)	11.4 (3)

Table 2
Comparison of hydrogen-bond parameters (Å, °) in (I) and (II).

Cg represents the centroid of the C101–C106 ring.

Compound	D—H···A	D—H	H···A	D···A	D—H···A
(I)	C3—H3···O5^{i}	0.95	2.60	3.548 (3)	176
(II)	C72—H72···N11^{ii}	0.95	2.62	3.395 (3)	139
	C104—H104···O6^{iii}	0.95	2.45	3.114 (3)	127
	C75—H75···*Cg*^{iv}	0.95	2.89	3.636 (2)	168

Symmetry codes: (i) $-x, y+\frac{1}{2}, -z-\frac{1}{2}$; (ii) $-x+1, -y+1, -z+1$; (iii) $x, y, z+1$; (iv) $-x+1, -y, -z+1$.

For both compounds, data collection: *COLLECT* (Nonius, 1999); cell refinement: *DIRAX*/*LSQ* (Duisenberg *et al.*, 2000); data reduction: *EVALCCD* (Duisenberg *et al.*, 2003). Program(s) used to solve structure: *SHELXS97* (Sheldrick, 2008) for (I); *SIR2004* (Burla *et al.*, 2005) for (II). For both compounds, program(s) used to refine structure: *SHELXL97* (Sheldrick, 2008); molecular graphics: *PLATON* (Spek, 2009); software used to prepare material for publication: *SHELXL97* and *PLATON*.

The authors thank the Centro de Instrumentación Científico-Técnica of the Universidad de Jaén and the staff for data collection. YD and JQ thank COLCIENCIAS, Universidad del Valle, for financial support. JC thanks the Consejería de Innovación, Ciencia y Empresa (Junta de Andalucía, Spain), the Universidad de Jaén (project reference UJA_07_16_33) and the Ministerio de Ciencia e Innovación (project reference SAF2008-04685-C02-02) for financial support.

Supplementary data for this paper are available from the IUCr electronic archives (Reference: GZ3177). Services for accessing these data are described at the back of the journal.

References

Allen, F. H., Kennard, O., Watson, D. G., Brammer, L., Orpen, A. G. & Taylor, R. (1987). *J. Chem. Soc. Perkin Trans. 2*, pp. S1–19.
Bell, M. R. & Ackerman, J. H. (1990). US Patent No. 4 920 128.
Bernstein, J., Davis, R. E., Shimoni, L. & Chang, N.-L. (1995). *Angew. Chem. Int. Ed. Engl.* **34**, 1555–1573.
Bristol–Meyers Co. (1973). Fr. Patent No. 2 149 275.
Burla, M. C., Caliandro, R., Camalli, M., Carrozzini, B., Cascarano, G. L., De Caro, L., Giacovazzo, C., Polidori, G. & Spagna, R. (2005). *J. Appl. Cryst.* **38**, 381–388.

Chen, Y., Wu, S., Tu, S., Shi, F. & Li, C. (2008). *J. Heterocycl. Chem.* **45**, 1243–1246
Day, G. M. *et al.* (2009). *Acta Cryst.* B**65**, 107–125.
Duisenberg, A. J. M., Hooft, R. W. W., Schreurs, A. M. M. & Kroon, J. (2000). *J. Appl. Cryst.* **33**, 893–898.
Duisenberg, A. J. M., Kroon-Batenburg, L. M. J. & Schreurs, A. M. M. (2003). *J. Appl. Cryst.* **36**, 220–229.
Farghaly, A. M., Habib, N. S., Khalil, M. A. & El-Sayed, O. A. (1989). *Alex. J. Pharm. Sci.* **3**, 90–94.
Ferguson, G., Glidewell, C., Gregson, R. M. & Meehan, P. R. (1998*a*). *Acta Cryst.* B**54**, 129–138.
Ferguson, G., Glidewell, C., Gregson, R. M. & Meehan, P. R. (1998*b*). *Acta Cryst.* B**54**, 139–150.
Gatta, F., Pomponi, M. & Marta, M. (1991). *J. Heterocycl. Chem.* **28**, 1301–1307.
Gregson, R. M., Glidewell, C., Ferguson, G. & Lough, A. J. (2000). *Acta Cryst.* B**56**, 39–57.
Nonius (1999). *COLLECT*. Nonius BV, Delft, The Netherlands.
Sheldrick, G. M. (2003). *SADABS*. Version 2.10. University of Göttingen, Germany.
Sheldrick, G. M. (2008). *Acta Cryst.* A**64**, 112–122.
Spek, A. L. (2009). *Acta Cryst.* D**65**, 148–155.